



Development of tribenzamide functionalized electrochemical sensor for femtomolar level sensing of multiple inorganic water pollutants

Tayyaba Kokab^a, Alia Manzoor^{a,***}, Afzal Shah^{a,b,**}, Humaira Masood Siddiqi^a, Jan Nisar^c, Muhammad Naem Ashiq^d, Aamir Hassan Shah^{e,*}

^a Department of Chemistry, Quaid-i-Azam University, Islamabad, 45320, Pakistan

^b Department of Chemistry, College of Science, University of Bahrain, Sakhir, 32038, Bahrain

^c National Centre of Excellence in Physical Chemistry, University of Peshawar, Peshawar, Pakistan

^d Institute of Chemical Sciences, Bahauddin Zakaryia University, Multan, 6100, Pakistan

^e Department of Chemistry and Biochemistry, University of California, Los Angeles, CA, 90095, USA

ARTICLE INFO

Article history:

Received 23 April 2020

Received in revised form

1 June 2020

Accepted 2 June 2020

Available online 6 June 2020

Keywords:

Electrochemical sensor

Femtomolar detection

Electrochemical characterizations

Limit of detection

ABSTRACT

A novel tribenzamides derivative *N*-(4-[2-(1,3-Benzoxazolyl)]phenyl)-3,5-*N,N'*-bis(4-hexyloxybenzoyl)benzamide (BOC6), containing three amide groups, was successfully synthesized and characterized through multiple spectroscopy techniques. The ultrasensitive electrochemical platform was developed by fabrication of glassy carbon electrode (GCE) with synthesized multifunctional tribenzamide appended BOC6 for the removal of water pollutants. The performance of the engineered sensor was studied by its electrochemical characterization with cyclic voltammetry (CV), electrochemical impedance spectroscopy (EIS), and square wave anodic stripping voltammetry (SWASV). The modifier played a facilitating role between the GCE surface and the target metal ions by bringing analytes closer to transducer surface resulting in appearance of intense electrochemical signals. Under pre-defined optimized conditions of SWASV, the BOC6 modified electrode was able to attain distinct oxidative current signals of thallium, arsenic, and mercuric ions simultaneously in one voltammogram scan. The sharp electrochemical signal and peak potential shift of thallium (Tl), arsenic (As) and mercury (Hg) oxidation at -0.79 V, -0.06 V and 0.22 V respectively, versus reference electrode Ag/AgCl evidence the electrocatalytic role of BOC6/GCE as compared to bare GCE at -0.68 V, -0.01 V and 0.3 V, respectively. Moreover, it was found to sense femtomolar concentration of aforementioned toxic ions, much lower than the world health organization (WHO) and environmental protection agency (EPA) guidelines for drinking water [1]. The limit of detections (LODs) obtained on for Tl(I), As(III), and Hg(II) detection were 2.19 fM, 1.97 fM, and 2.52 fM, respectively. Conclusively, the designed electrode was portable, cost effective, resistant to the interference species, highly stable and gives repeatable and reproducible voltammograms of analytes via strong interactions with target ions even in real water samples.

© 2020 Elsevier Ltd. All rights reserved.

1. Introduction

Heavy metals (HMs) like thallium, arsenic, mercury and their amalgams are highly toxic, ubiquitous in nature, non-biodegradable in environment, and can bio-accumulate in living

organisms via food chains [1]. Anthropogenic activities such as, rapid industrialization, disposal of municipal and industrial wastewater, mining, incineration, smelting, and agriculture are main sources of these contaminants [1]. These HMs are considerably hazardous to human health and water dwelling species even at minuscule level as declared by several international organizations such as, World Health Organization (WHO), Joint Food and Agricultural Organization (FAO), Centre for Disease Control (CDC), and Environmental Protection Agency (EPA) [2]. For instance, organic and inorganic arsenide's (As) toxicity lead to numerous diseases including, skin itching, keratosis, vomiting, nervous, cardiovascular, and respiratory system complications, bone marrow depression,

* Corresponding author.

** Corresponding author. Department of Chemistry, Quaid-i-Azam University, Islamabad, 45320, Pakistan.

*** Corresponding author.

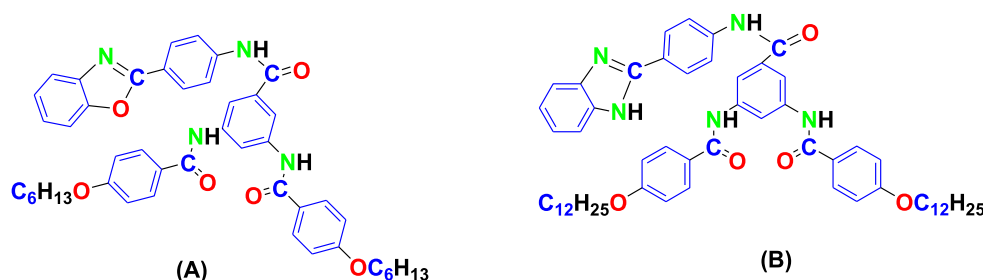
E-mail addresses: afzals_qau@yahoo.com (A. Shah), ah.shah@chem.ucla.edu (A.H. Shah).

cutaneous arsenicosis, and muscle cramps [3,4]. Furthermore, they can cause cancer of vital organs as identified by the International Agency for Cancer Research, IACR [2–9]. Likewise, the mercury (Hg) compounds are most frequently used in paintings, cosmetics, teeth filling, thermometers, barometers, blood pressure measuring instruments, and chloralkali industry etc. The mercury exposure can produce birth defects, respiratory system and gastrointestinal tract damages, autism, kidney malfunction, vestibular dysfunction, anxiety, speaking impairment, skin diseases, carcinogenic, mutagenic and teratogenic activities after crossing the threshold limit [7,10–14]. Similarly, thallium (Tl) is another heavy metal, which is even more toxic than mercury due to its high water solubility, bio-accumulation tendency, and susceptible entry to the body via potassium uptake pathways [14]. Correspondingly, thallium poisoning includes the alopecia, gastroenteritis, encephalopathy, polyneuropathy, peripheral and central nervous systems effects, tachycardia and degenerative changes of vital organs [14–18]. Moreover, amalgams of Tl forms eutectic alloys that have freezing point of $-60\text{ }^{\circ}\text{C}$ and have extensive applications in thermostatic devices [19]. However, in spite of high toxicity problems of these metal ions, their analysis and detection by conventional analytical methods is not feasible due to their poor responsiveness and low sensitivity at trace levels [20]. Additionally, these techniques have high cost and complicated instrumentation, time taking sample preparation and requirement of highly skilled operators [20]. Therefore, a simple ultrasensitive portable tool for their trace level sensing is urgently required to adopt effective measures in water reservoirs.

To develop new methods for better sensing and quantifying of such water pollutants, the stripping techniques and particularly square wave and differential pulse anodic stripping voltammetry (SWASV & DPASV) ensured alternative and extensive explored sensitive electrochemical methods for HMs ions detection [21]. Herein, the design of experiment (DOE) is based on primary voltammetric analysis (SWASV, CV and EIS) for the HM ions detection via cost-effective electrochemical computer-controlled workstation with advantages of simple electrode fabrication, portable handling, low voltage consumption and fast analysis. Moreover, anodic stripping voltammetry (ASV) is highly sensitive and selective due to electrochemical preconcentration/reduction of metal ions onto the surface of electrode and afterward subsequent anodic stripping steps [22,23]. Anodic stripping voltammetric (ASV) electrochemical sensor's performance is primarily required choice of some electroactive recognition materials on their working electrode that provide significant functionality to sensors along with boosting up their conductivity, stability, selectivity, surface area, and sensitivity [16,24]. Usually, electrocatalysts used for fabrication of sensors are surfactants, nanomaterials, polymers, carbon-based materials, organic ligands, and biomaterials [23,25,26]. However, HMs better analysis in water reservoir samples can be done via organic ligands that are robust complexing agents and are capable

to sequester these metal ions [13,19,27,28]. In recent advances of organic ligands based electroactive materials, the organic ligands having the amide functional moiety revealed strong and selective complexing ability towards metal ions when used to fabricate sensor [13,22,28,31] than other organic ligands [2,9,17,29,30]. For instance, they are vital constructing units of proteins, act as donor atoms in Ca^{2+} , Na^{+} , and K^{+} ions channels, and selectively use in the extraction and separation of precious metals and f-block elements through complexation with metal ions via O and N-donor potential binding sites of amide groups [25,32,33]. Considering their worthwhile bioactivity, benzamides and their synthesized oxazole, thiazole and imidazole derivatives having multi-functional electron releasing groups, have been registered to interact and chelate with metal ions to reduce them on sensor surface during accumulation step of ASV [34,35].

In this manuscript, we synthesized tribenzamide derivatives, *N*-{4-[2-(1,3-Benzimidazolyl)]phenyl}-3,5-*N,N'*-bis(4-dodecyloxybenzoyl)benzamide (BIC12) and *N*-{4-[2-(1,3-Benzoxazolyl)]phenyl}-3,5-*N,N'*-bis(4-hexyloxybenzoyl)benzamide (BOC6), that are designated as electroactive modifiers for the co-sensing of mercuric, arsenic, and thallium ions due to their metal ions complexing propensity (Scheme 1). Their coordinating ability and electrocatalytic role is credited to the electron donating benzamide tri-ring having amide moieties along with oxazoles, imidazoles, and ethers groups in its molecule [36–38]. These organic ligands are insoluble in aqueous solutions and thus stable on working electrode surface. Consequently, the fabricated sensors have high stability, viability and accuracy. Moreover, they possess electrode-anchoring hydrophobic groups and metal ion complexing agents like amides, oxazoles, imidazoles, and ethers that produce synergic effect for the coordination with metal ions and act as connecting bridge and facilitator between the sensor (host) and guest (target analytes) in the analyte's solution [35]. Likewise, they have highly accessible adsorption sites and non-agglomeration characteristics [34]. Furthermore, the BOC6 modified GCE revealed the better electrochemical sensing behavior in CV and SWASV for the co-sensing of mercury, arsenic, and thallium ions in water samples than BIC12, because heterocyclic organic ligands that have dissimilar donor atoms such as O–N type create more stable metal ion complexes than organic ligands having similar donor atoms like O–O, N–N types [35,39,40]. We have obtained six-fold high SWASV response for target analytes on BOC6/GCE than bare GCE on our DOE, which leads to high sensitivity of fabricated sensor. Because during pre-concentration step of SWASV, the amide group's presence in the tribenzamide molecules interact with metal ions and increase their absorptivity on electrode surface. The metal ions get reduced on BOC6/GCE surface by establish of coordinate covalent bonds with amide groups of tri-ring benzamide molecules and produce transition metal complexes. Thus, the increase of metal ions adsorptive sites and accumulated amount of reduced metals, by BOC6 electron donor groups



Scheme 1. (A) BOC6 and (B) BIC12 molecular structures.

leads to significant enhancement of sensitivity. Moreover, it was found to sense femtomolar concentration of Tl(I) 2.19 fM, As(III) 1.97 fM, and Hg(II) 2.52 fM ions which is much lower than the WHO and EPA guidelines for drinking water [1]. The designed electrode is resistant to the interference species and gives repeatable and reproducible voltammograms of analytes via strong interactions with target ions even in real water samples. The results infer novelty of this work based on superior figure of merits of tribenzamide-based sensor and its excellent stability. Surprisingly, no single report of such a cost-effective, simple, selective BOC6 based electrochemical device for the on-site simultaneous detection of these toxic ions at femtomolar level in aqueous medium is available in literature.

2. Experimental

2.1. Chemical reagents and real water samples

Synthetic details of BOC6 and BIC12 electrocatalysts are given in the succeeding section. All chemicals of analytical grade were procured from sigma Aldrich and Merck Germany and used without any purification steps. While, arsenic chloride, thallium sulphate and mercuric chloride were used to prepare analyte solutions. Strontium nitrate, zinc acetate, cesium chloride, cobalt chloride, calcium chloride, lead nitrate, alanine, lysine, threonine, glutamic acid, surfactants (CTAB, SDS), EDTA, glucose, citric acid, 2-amino-4-nitrophenol, and 3-chloro-5-nitrophenol were used to prepare interfering agents solutions. Acetic acid, sodium acetate, HCl, NaOH, sodium phosphate monobasic monohydrate, KCl, H₂SO₄, H₃BO₃, H₃PO₄, dimethyl sulphoxide (DMSO), and sodium phosphate dibasic heptahydrate were used to prepare supporting electrolytes solutions. The selection of the solvents was based on the solubility of analyte and tribenzamide compounds, doubly distilled water (ddw) was used for the preparation of metal ions, buffers and interferents solutions while the DMSO of the analytical grade was used for BOC6 and BIC12 solutions based on the insolubility of tribenzamide compounds in aqueous media. Glass apparatus was used after washing it with 6 M HNO₃ and then thoroughly rinsing it with ddw to prevent any metal contaminations. Real-life samples like tap water, drinking water, spring water, river water, soil wastewater, and industrial wastewater were obtained from different areas in Islamabad, Pakistan, in order to check the validity and applicability of our established sensor. These water samples were filtered through the Whatman filter paper No. 40 to remove soil particles or any other impurity before further use.

2.2. Instrumentation

Nuclear magnetic resonance (NMR) spectra were obtained from Bruker 300 MHz digital NMR instruments, Germany. Fourier transform infrared spectroscopy (FT-IR) spectra were obtained on Thermo Scientific Nicolet 6700 FTIR, U.S. Melting point (M.P) of the synthetic tribenzamide samples were obtained on m.p apparatus of Mel-Temp, Mitamura Riken Kogyo, Inc. Tokyo Japan. The EDX analysis along with SEM were carried out on ZEISS EVO 40 (Merlin, Carl Zeiss) for morphological characterization of sensor. Design of experiment (DOE) that is, voltammetric measurements (ASV, CV and EIS) were carried out on electrochemical computer-controlled workstation Metrohm Auto lab (PGSTAT 302N), Switzerland with general three electrode scheme as shown in Figure S1. Moreover, an INOLAB pH meter, Xylem Analytics Germany was used to set pH values of the buffers and working solutions. Glassy carbon electrode (GCE) of 0.071 cm² active area was employed as working electrode (WE), whereas Ag/AgCl (concentrated KCl) and Platinum

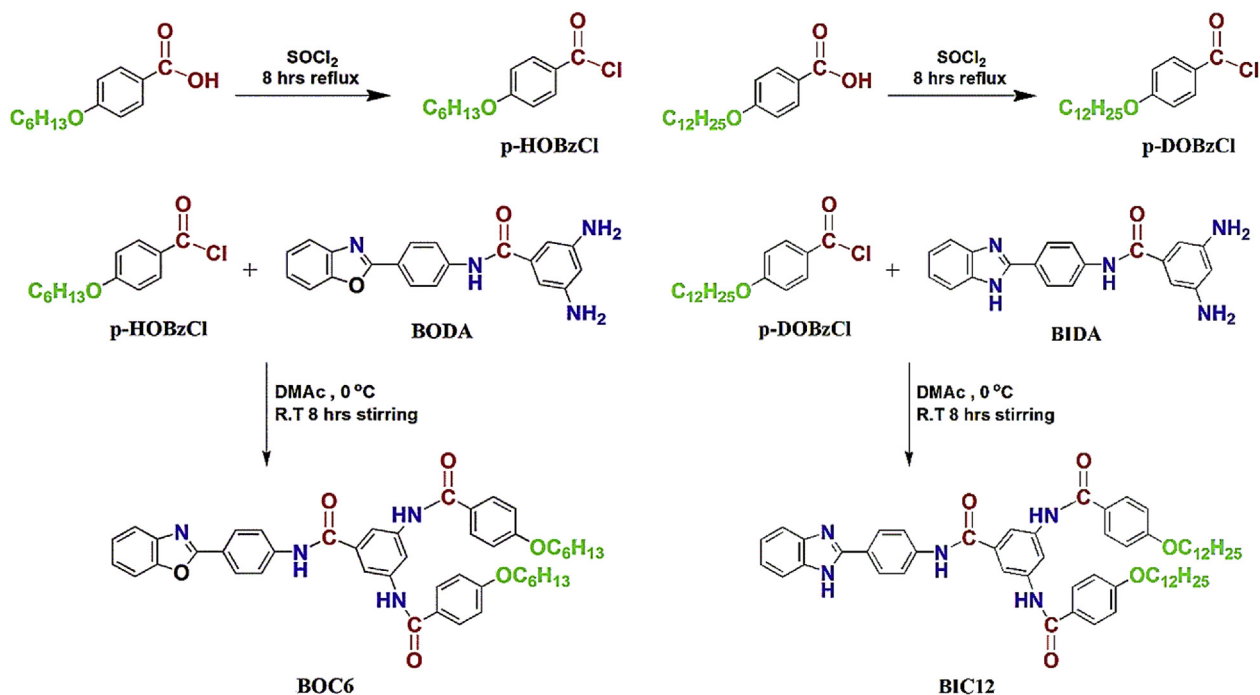
wire were used as reference (RE) and counter electrode (CE), respectively. WE and RE were set at nearby distance in the electrochemical cell to avoid ohmic/IR drop. All electrochemical studies were done at the room temperature (25 ± 2 °C) under inert atmosphere in order to evacuate the atmospheric oxygen by continuous purging of N₂ gas.

2.3. Synthesis and structural confirmations of tribenzamide derivatives

Tribenzamide derivative BOC6 was synthesized by reacting freshly prepared diamines N-(1,3-benzoxazol-2-ylphenyl)-3,5-diaminobenzamide (BODA) and p-hexyloxybenzoyl chloride (p-HOBzCl) according to the reported procedure [41]. The general steps involved in the synthesis of BOC6 are presented in Scheme 2. Firstly, p-hexyloxybenzoic acid (40 mmol) and thionyl chloride (8 mL) were mixed and set at 6 h continuous reflux in an oil bath to get the p-hexyloxybenzoyl chloride. Excess thionyl chloride was recovered by vacuum distillation after completion of the reaction. Secondly, 20 mmol solution of BODA in dimethylacetamide (DMAC) was added dropwise in reaction flask at 0 °C via dropping funnel. This solution was mixed for 8 h to get the final product of BOC6. In order to observe the reaction proceedings, TLC was performed at 25 °C by using n-hexane and ethyl acetate in 1:4. After completion of the reaction, the whole mixture was decanted into doubly distilled water to filter the product. The product was purified with excess water and then repeatedly recrystallized in alcohol, ethyl acetate, and THF, respectively. Moreover, second tribenzamide derivative BIC12 was formed by the same process using freshly prepared diamine N-(1,3-benzimidazol-2-ylphenyl)-3,5-diaminobenzamide (BIDA) and p-dodecyloxybenzoyl chloride (p-DOBzCl) reaction as shown in Scheme 2. Synthesized BOC6 and BIC12 were obtained in powder form with 82% and 90% yields, respectively.

BOC6: R_f = 0.40, M.P. 183–185 °C; FTIR (ν_{max}, cm⁻¹): 3304 (N–H amide stretch), 3008 (C_{sp}–H stretch), 2920, 2850 (C_{sp}³–H stretch), 1671 (C=O stretch), 1607 (C=C aromatic bend), 1245 (C–O stretch). ¹H NMR (DMSO-d₆ δ ppm, 300 MHz): 0.85 (6H, t, J = 6.9 Hz, 15, 15'), 1.28 (6H, m, 12, 12'-14, 14'), 1.74 (4H, quin, J = 6.6 Hz, 11, 11'), 4.02 (4H, t, J = 6.6 Hz, 10, 10'), 6.96 (4H, d, J = 7.8 Hz, 9, 9'), 7.06 (2H, d, J = 8.6 Hz, 2, 2'), 7.40 (2H, d, J = 8.2 Hz, 3, 3'), 7.75 (2H, d, J = 8.5 Hz, 1, 1'), 7.85 (4H, m, 4, 4'; 8, 8'), 8.01 (2H, s, 6, 6'), 8.24 (1H, s, 7), 10.36 (3H, s, 5, 5', 5''); (Figure. S2 and S3) ¹³C NMR (DMSO-d₆ δ ppm, 300 MHz): 14.34 (C, 26), 22.50 (C, 25), 25.59 (C, 24), 28.93 (C, 23), 31.40 (C, 22), 68.22 (C, 21), 110.02 (C, 1), 111.23 (C, 14, 14'), 114.53 (C, 19, 19', 19'', 19'''), 114.65 (C, 16), 120.03 (C, 4), 120.54 (C, 10, 10'), 123.17 (C, 2), 124.03 (C, 3), 125.78 (C, 8, 17, 17'), 128.40 (C, 9, 9'), 130.16 (C, 13, 18, 18', 18''), 131.81 (C, 11, 15, 15'), 142.05 (C, 5), 150.60 (C, 6), 161.98 (C, 20, 20'), 162.76 (C, 7), 167.53 (C, 12, 12', 12'') (Figure. S4).

BIC12: R_f = 0.70, M.P. 199–201 °C; FTIR (ν_{max}, cm⁻¹): 3343 (N–H amide stretch), 3050 (C_{sp}–H stretch), 2920, 2850 (C_{sp}³–H stretch), 1680 (C=O stretch), 1608 (C=C aromatic bend), 1250 (C–O stretch). ¹H NMR (DMSO-d₆ δ ppm, 300 MHz): 0.82 (6H, t, J = 6.9 Hz, 22, 22'), 1.23 (18H, m, 13, 13'-21, 21'), 1.75 (4H, quin, J = 6.6 Hz, 12, 12'), 4.01 (4H, t, J = 6.6 Hz, 11, 11'), 6.97 (4H, d, J = 8.8 Hz, 10, 10'), 7.39 (2H, d, J = 8.7 Hz, 2, 2'), 7.42 (2H, d, J = 8.4 Hz, 4, 4'), 7.76 (2H, d, J = 8.6 Hz, 1, 1'), 7.88 (4H, m, 5, 5', 9, 9'), 8.04 (2H, s, 7, 7'), 8.22 (1H, s, 8), 10.80 (3H, s, 6, 6', 6''), 12.80 (1H, s, 3); (Figure. S5 and S6) ¹³C NMR (DMSO-d₆ δ ppm, 300 MHz): 14.41 (C, 29), 22.57, 25.89, 28.98, 29.19, 29.49, 31.77 (C, 19, 19'), 68.19 (C, 18, 18'), 111.23 (C, 11, 11'), 114.62 (C, 16, 16', 16'', 16'''), 115.13 (C, 1, 1'), 120.08 (C, 13), 121.09 (7, 7'), 123.21 (C, 2, 2'), 125.28 (C, 5, 14, 14'), 128.59 (C, 6, 6'), 130.32 (C, 10, 15, 15', 15''), 131.78 (C, 8, 12, 12'),



Scheme 2. Representation of synthetic route for the tribenzamide derivative BOC6 and BIC12.

142.15 (C, 3, 3'), 150.63 (C, 4), 162.74 (C, 17, 17'), 167.45 (C, 9, 9', 9'') (Figure. S7).

2.4. Fabrication and electrochemical measurements of working electrode

For cleaning of GCE, firstly it was physically clean on a nylon polishing pad with μ -alumina slurry to get shiny surface by up to 14% constant O/C ratio [42]. Then, it was ultrasonicated for 5 min in ddw, alcohol and aq. HNO_3 (1:1, v/v). In the second step, electrochemical cleaning of GCE was performed by dipping it in PBS and taking several scans of cyclic voltammogram from -1.4 V to $+0.9$ V until reproducible cyclic voltammograms are obtained (Figure S8A).

Fabrication of WE was then performed at perfectly cleaned and activated GCE having 0.07 cm^2 active surface area, by casting 5 μL drop of the 10 μM synthetic tribenzamide solution in DMSO followed by drying in vacuum oven to ensure proper adsorption of modifier and to avoid non-uniformity in recognition layers. Furthermore, loosely bound molecules were stripped off by careful rinsing of the modified GCE with ddw.

At the GCE surface typically number of chemical functionalities i.e. aldehydes, ketones, carboxylic acids, quinones, lactones, and alcohols are found in configuration of fused aromatic rings which cause electrons delocalization throughout the carbon network that contribute to its O/C ratio [43]. The activation of GCE surface by physicochemical process improve its surface O/C ratio which mean the number of chemical functionalities increase on activated GCE surface. The casted tribenzamides molecules interact with them and get attached on the activated GCE surface as uniform recognition layer. During the electrode fabrication process, strong van der Waals forces result in tight binding of their hydrophobic electrode-anchoring tails to the GCE surface. Consequently, their metal ion complexing moieties become freely available for the electron transfer and Lewis acid-base interactions with target cations. The superficial description and elemental analysis of fabricated sensor on SEM and EDX provided in supporting information

section (Figure S8).

2.5. SWASV of fabricated electrodes

The bare, BOC6, and BIC12 sensors used as working electrodes and was dipped in electrochemical cell containing 1 μM of Tl^{1+} , 0.75 μM A^{3+} and 1.2 μM Hg^{2+} ions in 50% BRB solution at pH value of 5 as a stripping electrolyte. The metal ions were electro-reduced onto sensor surface at negative 1.2 V deposition potential for accumulation time of 135 s under continuous magnetic stirring. After that, the magnetic stir was stopped at equilibrium time of 5 s and the SWASV scan run from -1.3 V to $+0.6$ V at 20 mV pulse amplitude, 20 Hz frequency, 100 mVs^{-1} sweep rate, and 0.5 mV potential step. Hence, oxidative stripping of the metals from the sensor surface was occur in the quiescent solution and resultant well-resolved current peaks of metal ions was observe on voltammogram. For comparative purpose, SWASV electroplating and stripping analysis steps were also done on bare GCE under same experimental conditions. Moreover, for each reading a new recognition layer was immobilized on electrode to confirm the reproducibility of results.

3. Results and discussion

3.1. Tribenzamide modified GCE electrochemical characterizations

Cyclic voltammetry (CV) was carried out to characterize the BOC6 and BIC12 tribenzamide modified GCE designed sensor by probing current response of $[\text{Fe}(\text{CN})]^{3-/4-}$ redox couple compare to the bare GCE, by immersing the electrodes in 5 mM solution of the $\text{K}_3[\text{Fe}(\text{CN})_6]$ redox probe and a 0.1 M KCl stripping electrolyte. Fig. 1A shows obvious increase and displacement in electrochemical reversible signal of $[\text{Fe}(\text{CN})]^{3-/4-}$ redox couple at BOC6 and BIC12 immobilized GCE than bare GCE. The tribenzamides molecules offer more availability, electrocatalysis and faster electron transduction of ions at the surface of electrode due to their

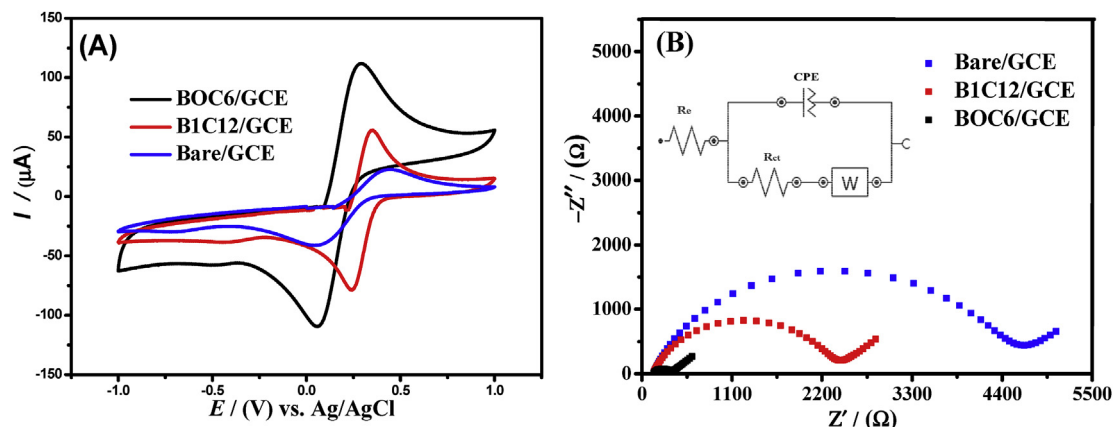


Fig. 1. Comparative plots obtained from bare GCE and tribenzamide-modified GCEs in a medium containing 5 mM $K_3[Fe(CN)_6]$ solution and a 0.1 M KCl electrolyte (A) Cyclic voltammograms at scan rate of 100 mV/s from potential -1.0 V– 1.0 V (B) Nyquist plots using electrochemical impedance spectroscopic data with applied DC voltage of 0 V vs. E_{OC} and amplitude of 10 mV over applied frequency ranges varying from 100 kHz to 0.1 Hz. (Inset) Randles equivalent circuit model for the system under study showing resistors, capacitor, and Warburg impedance elements.

excessive active sites for the redox probe accumulation on designed sensor. However, to calculate the large surface area of working electrode after modification with BOC6, the CV data was used in Randles-Sevcik equation of $I_p = 2.69 \times 10^5 n^{3/2} AD^{1/2} \nu^{1/2} C$. Where I_p represents the oxidative peak current in Amperes, n the number of electrons appearing in the half-reaction of probe, A the electroactive surface area in cm^2 , D the analyte diffusion coefficient in $cm^2 s^{-1}$, ν the scan rate at which the potential is swept in Vs^{-1} and C the concentration of the probe system in $mol cm^{-3}$ [44]. As cyclic voltammograms of bare GCE and tribenzamide-modified GCEs obtained in a medium containing 5 mM $K_3[Fe(CN)_6]$ solution and a 0.1 M KCl electrolyte at scan rate of 100 mV/s that's why $D = 7.6 \times 10^{-6} cm^2 s^{-1}$, $C = 5 mM$ and $n = 1$ were put in equation. The calculated areas of bare GCE, B1C12/GCE and BOC6/GCE were 0.02 cm^2 , 0.05 cm^2 and 0.095 cm^2 , respectively. Thus, after modification BOC6 tribenzamides the electroactive surface area of the modified GCE enhanced five times compared to bare electrode.

Similarly, the variation of designed sensor interfacial properties like, charge transfer features and extent of modification were analyzed via electrochemical impedance spectroscopy (EIS) in same solution [45]. In the EIS Nyquist plots, a semicircle diameter in the higher frequency region and a straight line in the lower frequency regime were obtained on bare GCE, BOC6 and B1C12 tribenzamide derivatives modified GCE. The semicircle arc region corresponds to charge transfer resistance (R_{ct}) at electrode/analyte interface and the linear line corresponds to the Warburg diffusion region as shown in Fig. 1B. The EIS data was fitted by the Randles equivalent circuit (inset of Fig. 1B) and attained parameters values were sum up in Table 1. The diameter of the semicircle that corresponds to the charge transfer resistance, is significantly smaller in case of BOC6/GCE and B1C6/GCE as compared to the bare GCE that corresponds to the facilitated charge transfer kinetics with effect of the tribenzamides fabrication. The R_{ct} value calculated for the BOC6 modified GCE ($R_{ct} = 0.21 k\Omega$) is quite low as compared to the B1C12

modified GCE ($R_{ct} = 2.2 k\Omega$), and the bare GCE ($R_{ct} = 4.35 k\Omega$) which confirmed that the recognition layer of the BOC6 indeed improves the sensing properties of the electrode by increasing the accessible active sites and the providing faster charge transductions.

The electrocatalytic role and sensing ability of the electroactive modifier corresponds to a kinetic parameter, exchange current density (J_0), which is inversely related to the R_{ct} value of EIS data via equation $J_0 = \frac{RT}{nFR_{ct}}$. Higher J_0 value associates to the remarkable electrocatalytic function of the recognition layer and its feasibility towards the interfacial surface electrochemical reactions. Thus, the higher exchange current density of the tribenzamide BOC6 modified GCE (127.5 $\mu A/cm^2$) as listed in Table 1, is attributed to its enhanced heterogeneous electrocatalysis and feasible redox reactions at BOC6/GCE surface [46].

3.2. Voltammetric analysis of modifier-metal ions complexation effect

The amide group is a bidentate ligand that forms a stable chelating tri-ring in the BOC6 and B1C12 tribenzamides and has strong affinity for the metal ions chelation. Hence, the BOC6 and B1C12 tribenzamides complexation effect on the modified electrodes performance for co-sensing of target triple ions was determined by CV in solutions of Tl^{1+} , As^{3+} and Hg^{2+} ions with a Britton–Robinson buffer (BRB) of pH 5 supporting electrolyte at sweep rate of 100 mV/s. The current intensity variation of Tl^{1+}/Tl^0 , As^{3+}/As^0 and Hg^{2+}/Hg^0 redox couples show noticeable current increase and potential shift in CV of the tribenzamides immobilized GCE compared to bare GCE as indicated in Fig. 2A. The enhancement further confirms the EIS results and attributed to the tribenzamide molecules that provide effective active sites and an increased surface area on the electrode surface for accumulation of the reduced metal ions [32]. Furthermore, the CV profile revealed reversibility of the design sensor and it can recognize the oxidized and reduced forms of target triple ions clearly. These results confirm the reversible interactions between host and guest i.e. complexation and decomplexation process of metal ions at sensor surface during run of an electrochemical scan. Moreover, the further enhancement of the current signals in case of the BOC6/GCE as compared to B1C12/GCE specify that the BOC6 molecules facilitate the redox probe approachability to the electrode surface better than the B1C12 molecules. This facilitation can be related to the difference of electroactive groups present in the BOC6 and B1C12

Table 1
Randles circuit parameters calculated for bare and tribenzamide modified GCEs from electrochemical impedance spectroscopy (EIS).

Electrodes	R_{ct} (k Ω)	R_e (Ω)	CPE (μF)	J_0 ($\mu A/cm^2$)
GCE	4.35 ± 0.04	198.2 ± 1.58	3.63 ± 0.12	5.9
B1C12/GCE	2.2 ± 0.01	142.2 ± 1.2	2.38 ± 0.10	11.7
BOC6/GCE	0.21 ± 0.05	139 ± 1.3	1.52 ± 0.23	127.5

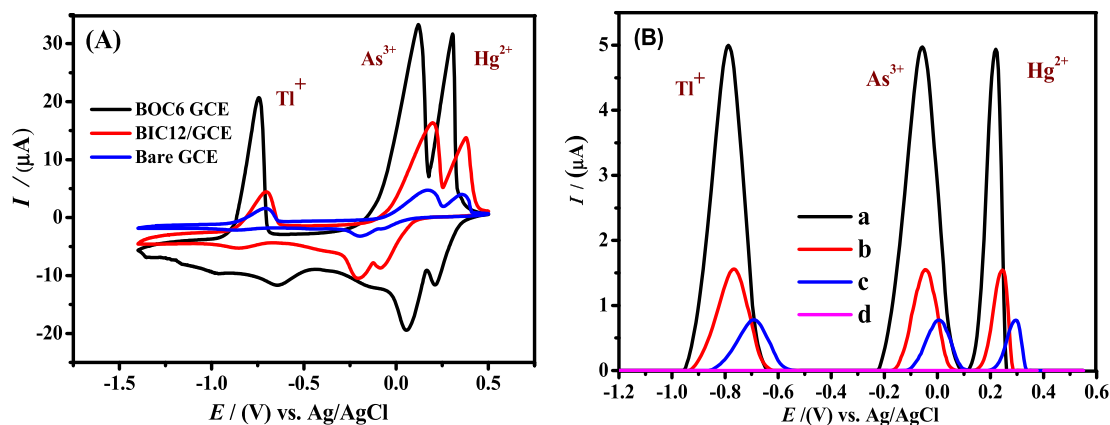


Fig. 2. (A) Cyclic voltammograms of Tl^{1+} , As^{3+} and Hg^{2+} ions at scan rate of 100 mV/s from working potential -1.3 V– 0.5 V (B) SWASVs obtained from a) BOC6 modified GC electrode, b) BIC12 modified GC electrode, and c) bare GC electrode for the detection of $1 \mu\text{M}$ of Tl^{1+} , $0.75 \mu\text{M}$ As^{3+} and $1.2 \mu\text{M}$ Hg^{2+} ions in BRB of pH = 5 as stripping solvent, keeping a scan rate of 100 mV/s, a deposition potential of -1.2 V and a deposition time of 135 s d) The BOC6 designed sensor in aqueous solvent containing BRB (pH 5.0) under same experimental conditions.

molecular structures and their molecular geometries. The BIC12 possesses bulky molecular structure as shown in Scheme 1, that offers more structural hindrance for the analyte's interaction on the electrode surface as compared to the BOC6. Likewise, the tribenzamide BOC6 has more hetero-atomic electron donating groups with more electronegative units and interact better with the metal cations. Consequently, BOC6 is better electrochemical device for the co-sensing of Tl^{1+} , As^{3+} and Hg^{2+} ions as compared to BIC12 [36–38].

The SWASVs were recorded at the tribenzamide modified electrodes (BOC6/GCE & BIC12/GCE) for $1 \mu\text{M}$ of Tl^{1+} , $0.75 \mu\text{M}$ As^{3+} and $1.2 \mu\text{M}$ Hg^{2+} ions to further assess their electrochemical performance in terms of sensitivity and selectivity toward the target analytes as shown in Fig. 2B. The SWASV oxidative signatures of Tl^{1+} , As^{3+} and Hg^{2+} metal ions on the BOC6 & BIC12 modified electrodes significantly shifted to the more negative potential than the bare GCE, which indicate the electrocatalytic role of these tribenzamide derivatives via their electroactive sites. Moreover, in SWASV a noticeable approximately six folds and two folds' amplification of the oxidative signal intensity of Tl^{1+} , As^{3+} and Hg^{2+} ions, was seen at the BOC6 and BIC12 immobilized GCEs, respectively than the bare GCE. At fabricated GCE surface, the modifier molecule configure itself in such a way that its chelating moieties are freely available to interact with the aqueous target analytes [43]. Therefore, the enhancement of Tl^{1+} , As^{3+} and Hg^{2+} ions peak current intensity can be related to the contribution of the amide groups present in the tri-ring of the modifiers and metal ions complexation (that increase their electroplating efficacy in the accumulation step of SWASV). Likewise, the ether, imidazole, and oxazole electron-rich functionalities of the recognition layers also offer adsorption sites for the metal cations to form $\text{M}/\text{M}^{\text{X}+}$ couple and, enhanced their current responses by serving as a venturing stone between the host and guest for faster electron transfers [47]. These SWASV results are in good agreement with the electrochemical characterizations mentioned in the outcomes of designed sensors and confirm their electrocatalytic sensing mechanism via complexation-decomplexation process. Based on these results, the BOC6/GCE was selected as an electrochemical sensor of Tl^{1+} , As^{3+} and Hg^{2+} ions detection in all onward electrochemical investigations. The optimization of the parameters like modifier concentration, stripping electrolyte and its pH values, deposition times, and accumulation potentials on the sensing sensitivity, shape, and intensity of the metal ions current signals at BOC6/GCE are provided in Supporting information section.

3.3. Evaluation of analytical features

Under the pre-optimized SWASV conditions (supporting information), the linear concentration ranges (LCRs), limit of detection (LOD) and limit of quantification (LOQ) of the BOC6/GCE sensor were investigated for the co-sensing of Tl^{1+} , As^{3+} and Hg^{2+} ions. A robustness in analytical response of the sensor was observed in the voltammograms obtain at investigated concentration ranges of 0.05 pM – $0.15 \mu\text{M}$, 0.025 pM – $0.125 \mu\text{M}$, and 0.075 pM – $0.175 \mu\text{M}$ of the $\text{Tl}(\text{I})$, $\text{As}(\text{III})$, and $\text{Hg}(\text{II})$ respectively, as shown in Fig. 3A. The linear calibration curves were obtained by plotting oxidative peak current values of the Tl^{1+} , As^{3+} and Hg^{2+} ions from the SWASVs versus their concentrations. The LCRs for Tl^{1+} , As^{3+} and Hg^{2+} ions were determined in the range of 0.05 pM – 37.5 nM , 0.025 pM – 25 nM and 0.075 pM – 50 nM with correlation coefficients R^2 of 0.997, 0.995, and 0.997 respectively, as shown in Fig. 3B. The LODs values for Tl^{1+} , As^{3+} and Hg^{2+} ions were assessed by their IUPAC regulations and found 2.19 fM , 1.97 fM , and 2.52 fM respectively. Likewise, the LOQs for Tl^{1+} , As^{3+} and Hg^{2+} were obtained as 7.3 fM , 6.56 fM , and 8.4 fM respectively. The lower LODs are related to the better sensitivity and higher current response of the BOC6/GCE. Comparatively LOD of 1.97 fM for arsenic ions at the BOC6/GCE under pre-defined SWASV conditions was the lowest than thallium (2.19 fM) and mercury (2.52 fM) ions. This enhance response of the sensor for arsenic ions can be related to its smaller radius with high charge density and thus greatest tendency for interaction and complex formation with the modifier. Henceforth, it is concluded that the BOC6 is more selective and sensitive for complexation with arsenic than other target analytes, but at the same time, it possesses better sensing ability and offers effective interactions for all metal cations under investigation.

3.4. Reproducibility and repeatability of the BOC6 sensor

The stability, durability, and repeatability of the BOC6/GCE was probed by recording eight successive SWASVs at different intervals of times for $0.15 \mu\text{M}$ of Tl^{1+} , $0.125 \mu\text{M}$ As^{3+} and $0.175 \mu\text{M}$ Hg^{2+} ions at a single BOC6/GC electrode under the constant pre-defined optimum experimental conditions. After intra and inter day repetitive measurements as illustrated in Fig. 4A, the obtained voltammetric signals demonstrate the analogous responses with RSD of 2.1%, 1.84%, and 1.36% for Tl^{1+} , As^{3+} and Hg^{2+} ions, respectively. Thus, the developed sensor shows outstanding stability over a long period of storage time due to its insolubility in aqueous solutions.

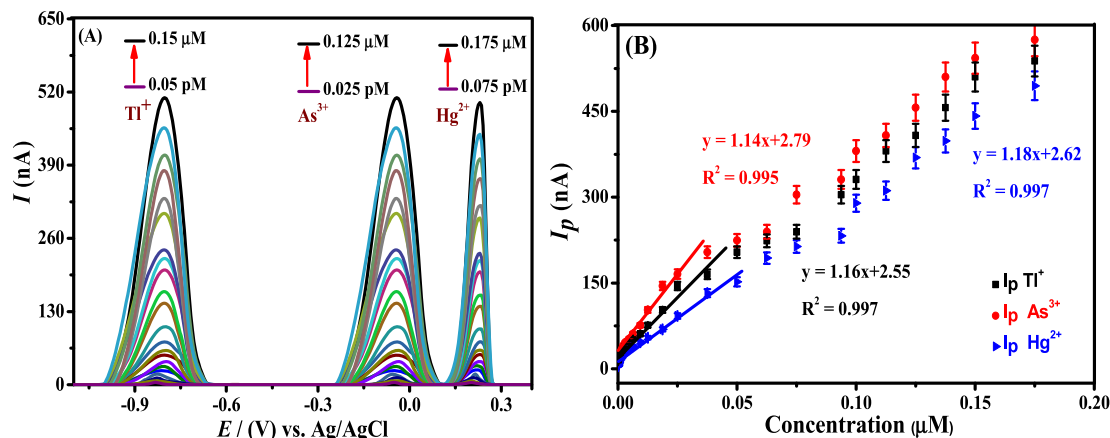


Fig. 3. (A) SWASV recorded at BOC6/GCE by varying concentrations of Tl^{1+} , As^{3+} and Hg^{2+} ions in BRB (pH = 5), a scan rate of 100 mV/s, a deposition potential -1.2 V, and a deposition time of 135 s. The investigated concentration ranges are mentioned above each peak. (B) The corresponding calibration plots with error bars, linearity ranges and linear equations, obtained by SWASV data, showing linearity of Tl^{1+} , As^{3+} and Hg^{2+} ions concentration with I_p under optimized conditions used for sensitivity, applicability and validity of BOC6/GCE for multiple ions detection.

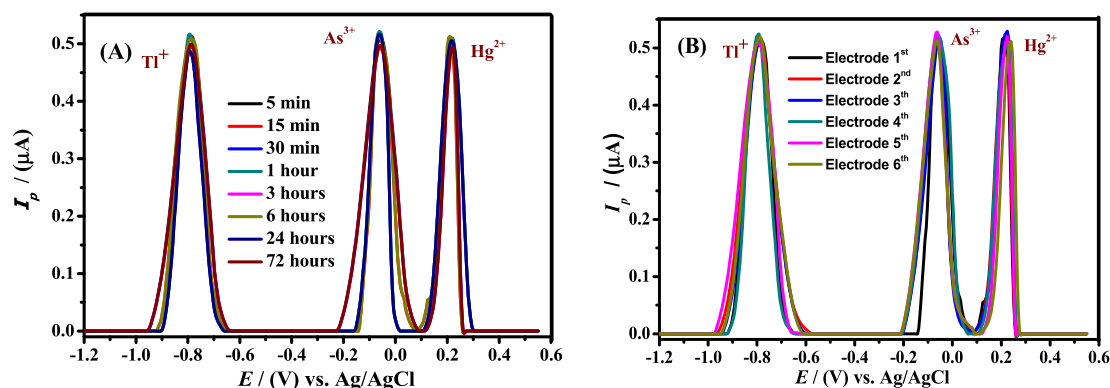


Fig. 4. Validation of the applied methodology testified by monitoring the SWASV peak current responses for $0.15 \mu M$ of Tl^{1+} , $0.125 \mu M$ As^{3+} , and $0.175 \mu M$ Hg^{2+} ions solutions under optimized conditions; (A) showing repeatability of the designed BOC6/GCE electrode at intra and inter days scans obtained at electrode dipped time mentioned in figure ($n = 8$), (B) showing reproducibility of multiple fabricated BOC6/GCE electrodes ($n = 6$).

Likewise, in an attempt to assess the reproducibility of the devised sensor, six independently BOC6 fabricated electrodes were used for the successive scans of SWASV for the electrodeposited Tl, As, and Hg metals as shown in Fig. 4B. No obvious inconsistencies in the oxidation peak signatures of $0.15 \mu M$ of Tl^{1+} , $0.125 \mu M$ As^{3+} and $0.175 \mu M$ Hg^{2+} ions were found with RSD of 1.50%, 1.53%, and 1.71%. These outcomes elucidate noteworthy reproducibility and repeatability of the developed electrochemical sensor and hence, render it an ultrasensitive reliable platform for HM ions detection. The figure of merits (FOM) of the designed sensor of the BOC6 tribenzamide

derivative is summarized in Table 2, suggesting the promising properties of our tribenzamide based electroanalytical sensor.

Furthermore, these calculated FOMs such as LOD values are much lower than WHO and USEPA recommended threshold limits, and also from those sensors already reported in the literature for detection of Tl^{1+} , As^{3+} and Hg^{2+} ions [1–7,10–14,16–18,30,35]. Briefly, in comparative Table 3, the LODs of previously reported graphene oxides, carbon nanotubes, precious metals nanoparticles and nanocomposites, silica, amines, and polymers fabricated sensors for Tl^{1+} , As^{3+} and Hg^{2+} ions detection are significantly inferior

Table 2

Figures of merits of the BOC6 modified GCE for Tl^{1+} , As^{3+} and Hg^{2+} ions.

Figures of merits	Units	Tl^{1+}	As^{3+}	Hg^{2+}
Investigated range	μM to pM	0.15–0.05	0.125–0.025	0.175–0.075
Linearity range	nM to pM	37.5–0.05	25–0.025	50–0.075
LOD	fM	2.19	1.97	2.52
LOQ	fM	7.3	6.56	8.4
% RSD (Reproducibility)	n=6	1.50	1.53	1.71
% RSD (Repeatability)	n=8	2.1	1.84	1.36
% RSD (Validity)	n=6	1.02–1.96	1.02–2.05	0.96–2.02
% RSD (Anti-interference ability)	n=15	2.22	2.16	2.18
Recovery (%)	n=12	95–100	95–100	95–100

Table 3
Comparison of some figures of merit related to the different reported modified electrodes for the sensing ability of Tl^{1+} , As^{3+} and Hg^{2+} ions.

Sensors	Measurement technique	LOD (nM)			Ref.
		Tl^{1+}	As^{3+}	Hg^{2+}	
MEA/Au electrode ^a	DPASV	N.M ^b	20	N.M	[2]
Au NPs/CNTs/GCE	SWV	N.M	100	N.M	[3]
Au NPs/GCE	ASV	N.M	24	N.M	[4]
Au/MPS-(PDDA-AuNPs)	DPASV	N.M	480	N.M	[5]
Pt NPs/CNTs	LSV	N.M	1.6	N.M	[6]
layer-by-layer assembled DNA	LSV	N.M	0.67	N.M	[6]
[Ru(bpy) ₃] ²⁺ -GO/GCE	DPV	N.M	2.3	1.6	[7]
GC-IIP-MWCNTs	DPASV	N.M	N.M	5.0	[10]
Cu-CoHCF/GCE with L-Cysteine	DPV	N.M	N.M	80.0	[11]
IL/SBA 15-silica/CPE	DPASV	N.M	N.M	10.0	[12]
PPy/Pct/GR/GCE	DPASV	N.M	N.M	6×10^{-6}	[13]
Bi nanopowder electrode	SWASV	30	N.M	N.M	[13]
Gly/GCE	SWASV	0.175	N.M	0.23	[14]
Bi film electrode	SWASV	10.8	N.M	N.M	[16]
LB-p-allylcalix [4]arene/GCE	DPASV	5.0	N.M	N.M	[17]
IL/Gr/L/CPE	SWASV	6.01	N.M	N.M	[18]
4-MPY/Au NPs	SPR	N.M	N.M	8	[30]
ZE-2/GCE	SWASV	N.M	N.M	1.28	[35]
BOC6/GCE	SWASV	2.19×10^{-6}	1.97×10^{-6}	2.52×10^{-6}	This work

^a MEA/Au electrode = mercaptoethylamine modified Au electrode; Au NPs/CNTs = gold nanoparticles/carbon nanotubes (CNTs); Au/MPS-(PDDA-AuNPs) = poly(diallyldimethylammonium chloride) and citrate capped Au nanoparticles anchored on sodium 3-mercapto-1-propanesulfonate modified gold electrode; [Ru(bpy)₃]²⁺-GO = ruthenium(II) bipyridine complex-textured graphene oxide nanocomposite; IIP-MWCNTs = ion imprinted polymeric nanobeads and multi-wall carbon nanotubes; Cu-CoHCF = copper-cobalt hexacyanoferrate; IL/SBA 15-silica/CPE = ionic liquid-ordered mesoporous silica/carbon paste electrode; PPy/Pct/GR = polypyrrole, pectin and graphene nanocomposites; Gly = glycine; LB-p-allylcalix [4]arene = Langmuir-Blodgett (LB) film of p-allylcalix [4]arene; 4-MPY/Au NPs = mercaptopyrindine-functionalized gold nanoparticles; ZE-2 = Co-based zeolitic imidazolate framework (ZIF-67) and ex-panded graphite (EG); **BOC6** = Tribenzamide derivative.

^b N.M = not measured.

to our novel designed electroanalytical BOC6 fabricated sensor. These results infer superior properties of our tribenzamide-based sensor and its excellent stability.

3.5. Interference study for validation of sensor

In real matrices of water samples, commonly competitive redox species and complexing agents are present along with the target analytes that can be reduced on sensor surface and influence the sensing of focus HM ions in practical application of electrochemical sensors [25]. However, multiple co-existed cations can display their oxidation peaks on SWASVs at different stripping potentials under different experimental conditions. Therefore, it is necessitated to thoroughly investigate the various potential interferents effect on the sensor performance and its validity for Tl^{1+} , As^{3+} and Hg^{2+} ions detection. In this regard, the SWASVs of 0.15 μ M of Tl^{1+} , 0.125 μ M As^{3+} and 0.175 μ M Hg^{2+} ions in potential range from -1.2 V to 0.6 V at deposition potential of -1.2 V, was investigated in the presence of 2 mM concentration of organic and inorganic interfering species such as, 2-amino-4-nitrophenol, 3-chloro-5-nitrophenol, CS^+ , Ca^{2+} , Sr^{2+} , Co^{2+} , Pb^{2+} , K^+ , Zn^{2+} , EDTA, glucose, SDS, CTAB, amino acid and citric acid as displayed in voltammograms of Fig. 5A. Consequently, SWASVs electrochemical signals revealed that the presence of multi-fold higher amount of the interfering agents can slightly affect the metal ions oxidative peak currents under optimized conditions with RSD of 2.22%, 2.16%, and 2.18% for Tl^{1+} , As^{3+} and Hg^{2+} ions, respectively as shown in bar Figure 5Baph in. The multiple ions in the homogeneous BRB pH 5 electrolyte may have adsorption competition on the sensor surface depending on their concentrations and interactions toward modifier. Nevertheless, SWASVs results reveal no obvious discrepancy, this phenomenon might be attributed to enrichment of target triple ions on the designed sensor surface by qualifying the competition for accumulation sites because of strong binding affinity and complexation of the tribenzamide recognition layer. However, a

small signal of lead ions, with no significant deviation in target analytes signals was also observed. These results indicate that lead ions can also be detected and quantified by designed sensor, but at different experimental conditions. Hence, our devised electrochemical sensing platform possess signifying resistance to the interferences and capable to recognize the target analytes with absolute discrimination ability.

3.6. Practical applicability of sensor by study of real samples

To ensure the precision and practical applicability of the proposed method of the electrochemical sensing, the BOC6 modified GCE was applied for monitoring of Tl^{1+} , As^{3+} and Hg^{2+} ions in real sample matrixes under defined experimental conditions. For this purpose, the SWASV was performed in the electrochemical cell having a water sample with 50% of the BRB (pH = 5) to determine the initial concentration of Tl^{1+} , As^{3+} and Hg^{2+} ions in tap water, drinking water, spring water, river water, soil and industrial waste water samples. Afterward, by the conventional standard addition method, the known amount of metal ions from their stock solution was spiked in water sample and recovery tests were performed accordingly at the predefined experimental conditions of SWASV. The concentration of spiked ions was then evaluated from the linear calibration plot of I_p versus concentration and the recovery percentages extended from 95 to 100% with RSD of 0.96–2.05% are tabulated in Table 4. These results suggest the practical applicability, certain feasibility and precision of the suggested method for multi-metal ions detection.

4. Conclusion

In summary, we designed a novel tribenzamide derivative modified GCE and tested it for the recognizing of multiple toxic ions i.e. $Tl(I)$, $As(III)$, and $Hg(II)$ in water systems. At BOC6/GCE, low R_{ct} value in EIS, noticeable redox ions reversibility in CV, enhance

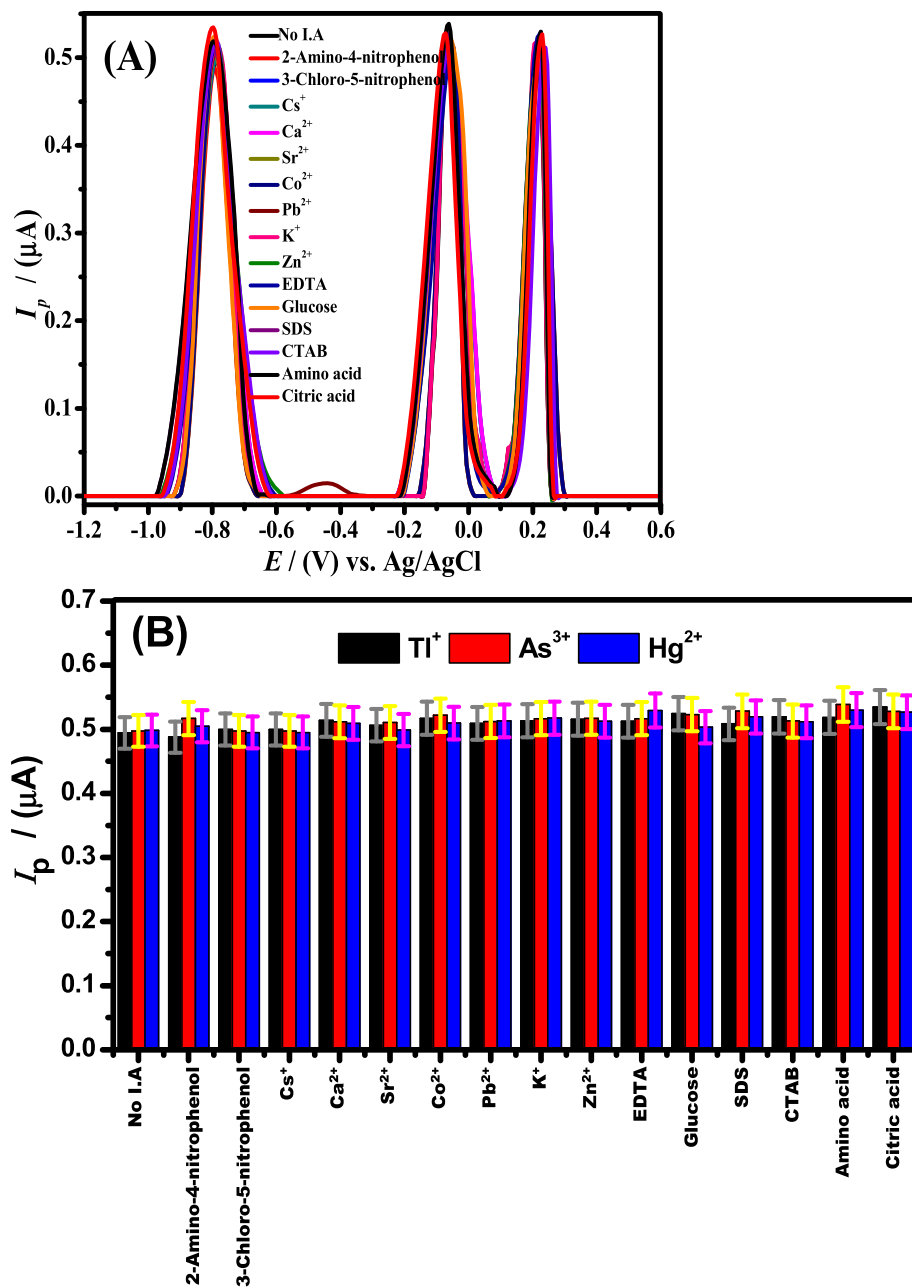


Fig. 5. (A) Voltammograms of metal analytes performed with a BOC6 modified electrode in the presence of 2 mM of one of the interfering agents i.e., 2-amino-4-nitrophenol, 3-chloro-5-nitrophenol, Cs^+ , Ca^{2+} , Sr^{2+} , Co^{2+} , Pb^{2+} , K^+ , Zn^{2+} , EDTA, glucose, SDS, CTAB, amino acid and citric acid in cell having $0.15 \mu\text{M}$ of Tl^+ , $0.125 \mu\text{M}$ As^{3+} and $0.175 \mu\text{M}$ Hg^{2+} ions in BRB of pH 5 under chosen optimized conditions. (B) Corresponding bar graph with error bar showing adsorptive stripping peak current I_p of Tl^+ , As^{3+} and Hg^{2+} ions SWASV effected by 2 mM concentrations of various organic and inorganic interfering agents.

target ions peak current intensity and negative potential shift in SWASVs, ensure that the fabricated working electrode offer faster electron transduction, better electrocatalysis and enhanced sensitivity. These improved characteristics of fabricated sensor are associated with availability of excessive adsorption sites on sensor surface that increase the effective surface area of electrode for target ions sensing. Furthermore, under optimized conditions of SWASV, significantly enhanced well-defined oxidation current signals of the target metals were achieved at the fabricated electrode as compared to the bare GCE. The recommended sensing platform has remarkable characteristics of low cost, easy

fabrication, portable and the ecological benign. The SWASVs results showed that the BOC6 modified GCE possess excellent repeatable, reproducible, electrocatalytic, ultrasensitive and the selective electrode surface. The wide LCRs for the target metal ions and LODs of 2.19 fM, 1.97 fM, and 2.52 fM for $\text{Tl}(\text{I})$, $\text{As}(\text{III})$, and $\text{Hg}(\text{II})$ ions respectively are far below than the limits set by USEPA and WHO [1]. In addition, the developed analytical protocol has efficacy for sequestering the environmental pollutant in real-life water matrices with excellent anti-interference ability, reliability, validity and stability.

Table 4
Results for Tl^{1+} , As^{3+} and Hg^{2+} ions determination in real water samples obtained under the optimum experimental conditions.

Metal ions	Sample	Initially found (nM)	Spiked amount (nM)	Found amount (nM)	RSD (%)	Recovery (%)	
Tl^{1+}	Drinking water 1	0.00	17.50	17.45	1.15	99.71	
	Drinking water 2	0.00	17.50	17.51	1.02	100.05	
	Tap water 1	0.00	17.50	17.47	1.05	99.83	
	Tap water 2	0.00	17.50	17.44	1.29	99.65	
	Spring water 1	0.00	17.50	17.52	1.36	100.11	
	Spring water 2	0.00	17.50	17.49	1.22	99.99	
	River water 1	0.00	17.50	16.87	1.96	96.4	
	River water 2	0.00	17.50	17.33	1.87	99.0	
	Industrial wastewater 1	0.0001	17.50	17.22	1.82	98.4	
	Industrial wastewater 2	0.00	17.50	16.98	1.69	97.0	
	Soil 1	0.00	17.50	16.70	1.01	95.4	
	Soil 2	0.00	17.50	17.43	1.62	99.6	
	As^{3+}	Drinking water 1	0.00	15.00	14.75	2.05	98.33
		Drinking water 2	0.00	15.00	14.50	1.02	96.66
Tap water 1		0.00	15.00	14.90	1.25	99.33	
Tap water 2		0.00	15.00	14.60	1.19	97.30	
Spring water 1		0.00	15.00	14.25	1.76	95.00	
Spring water 2		0.00	15.00	15.09	1.12	100.60	
River water 1		0.00	15.00	14.60	1.16	97.4	
River water 2		0.00	15.00	14.93	1.37	99.5	
Industrial wastewater 1		0.00	15.00	14.90	1.42	99.4	
Industrial wastewater 2		0.00	15.00	14.63	1.39	97.5	
Soil 1		0.00	15.00	14.37	1.51	95.8	
Soil 2		0.00	15.00	14.93	1.32	99.5	
Hg^{2+}		Drinking water 1	0.00	20.00	19.9	1.05	99.50
		Drinking water 2	0.00	20.00	19.5	1.12	97.50
	Tap water 1	0.00	20.00	19.0	1.50	95.00	
	Tap water 2	0.00	20.00	19.4	1.90	97.00	
	Spring water 1	0.00	20.00	19.3	1.96	96.50	
	Spring water 2	0.00	20.00	19.9	2.02	99.75	
	River water 1	0.00	20.00	19.88	0.96	99.4	
	River water 2	0.00	20.00	19.94	1.73	99.7	
	Industrial wastewater 1	0.01	20.00	20.08	1.12	100.4	
	Industrial wastewater 2	0.0008	20.00	20.10	1.90	100.5	
	Soil 1	0.00	20.00	19.56	1.42	97.8	
	Soil 2	0.00	20.00	19.30	1.51	96.5	

Declaration of competing interest

Authors declare no conflict of interest.

It is certified that all authors in this manuscript have contributed.

Acknowledgments

Dr. Afzal Shah acknowledges the support of Quaid-i-Azam University and Higher Education Commission of Pakistan for supporting this work.

Appendix A. Supplementary data

Supplementary data to this article can be found online at <https://doi.org/10.1016/j.electacta.2020.136569>.

References

- [1] R. Aruliah, A. Selvi, J. Theertagiri, A. Ananthaselvam, K.S. Kumar, J. Madhavan, P. Rahman, Integrated remediation processes towards heavy metal removal/recovery from various environments—a review, *Front. Environ. Sci.* 7 (2019) 66.
- [2] D. Li, J. Li, X. Jia, Y. Han, E. Wang, Electrochemical determination of arsenic (III) on mercaptoethylamine modified Au electrode in neutral media, *Anal. Chim. Acta* 733 (2012) 23–27.
- [3] L. Xiao, G.G. Wildgoose, R.G. Compton, Sensitive electrochemical detection of arsenic (III) using gold nanoparticle modified carbon nanotubes via anodic stripping voltammetry, *Anal. Chim. Acta* 620 (2008) 44–49.
- [4] M.M. Hossain, M.M. Islam, S. Ferdousi, T. Okajima, T. Ohsaka, Anodic Stripping Voltammetric detection of arsenic (III) at gold nanoparticle-modified glassy carbon electrodes prepared by electrodeposition in the presence of various additives, *Electroanalysis* (N.Y.N.Y.) 20 (2008) 2435–2441.
- [5] M.M. Ottakam Thotiyil, H. Basit, J.A. Sánchez, C. Goyer, L. Coche-Guerente, P. Dumy, S. Sampath, P. Labbé, J.-C. Moutet, Multilayer assemblies of polyelectrolyte–gold nanoparticles for the electrocatalytic oxidation and detection of arsenic(III), *J. Colloid Interface Sci.* 383 (2012) 130–139.
- [6] J. Wu, L.N. Yang, N. Song, J.R. Chen, Nanometer materials modified electrodes for detection of heavy metal ions by stripping voltammetry, *Appl. Mech. Mater.* 488–489 (2014) 129–132.
- [7] M.B. Gumpu, M. Veerapandian, U.M. Krishnan, J.B.B. Rayappan, Simultaneous electrochemical detection of Cd (II), Pb (II), as (III) and Hg (II) ions using ruthenium (II)-textured graphene oxide nanocomposite, *Talanta* 162 (2017) 574–582.
- [8] M. Baghayeri, M. Ghanei-Motlagh, R. Tayebee, M. Fayazi, F. Narenji, Application of graphene/zinc-based metal-organic framework nanocomposite for electrochemical sensing of As(III) in water resources, *Anal. Chim. Acta* 1099 (2019) 60–67.
- [9] S.-H. Wen, R.-P. Liang, L. Zhang, J.-D. Qiu, Multimodal assay of arsenite contamination in environmental samples with improved sensitivity through stimuli-response of multiligands modified silver nanoparticles, *ACS Sustain. Chem. Eng.* 6 (2018) 6223–6232.
- [10] H.R. Rajabi, M. Roushani, M. Shamsipur, Development of a highly selective voltammetric sensor for nanomolar detection of mercury ions using glassy carbon electrode modified with a novel ion imprinted polymeric nanobeads and multi-wall carbon nanotubes, *J. Electroanal. Chem.* 693 (2013) 16–22.
- [11] V.V. Sharma, D. Tonelli, L. Guadagnini, M. Gazzano, Copper-cobalt hexacyanoferrate modified glassy carbon electrode for an indirect electrochemical determination of mercury, *Sensor. Actuator. B Chem.* 238 (2017) 9–15.
- [12] P. Zhang, S. Don g, G. Gu, T. Huang, Simultaneous determination of Cd^{2+} , Pb^{2+} , Cu^{2+} and Hg^{2+} at a carbon paste electrode modified with ionic liquid-functionalized ordered mesoporous silica, *Bull. Kor. Chem. Soc.* 31 (2010) 2949–2954.
- [13] A.D. Arulraj, R. Devasenathipathy, S.-M. Chen, V.S. Vasantha, S.-F. Wang, Femtomolar detection of mercuric ions using polypyrrole, pectin and graphene nanocomposites modified electrode, *J. Colloid Interface Sci.* 483 (2016) 268–274.
- [14] A. Shah, A. Nisar, K. Khan, J. Nisar, A. Niaz, M.N. Ashiq, M.S. Akhter, Amino acid functionalized glassy carbon electrode for the simultaneous detection of thallium and mercuric ions, *Electrochim. Acta* 321 (2019) 134658.
- [15] G.-J. Lee, H. Lee, Y. Uhm, L. min ku, C.K. Rhee, Square-wave voltammetric determination of thallium using surface modified thick-film graphite

- electrode with Bi nanopowder, *Electrochem. Commun.* 10 (2008) 1920–1923.
- [16] E. Jorge, M. Neto, M. Rocha, A mercury-free electrochemical sensor for the determination of thallium (I) based on the rotating-disc bismuth film electrode, *Talanta* 72 (2007) 1392–1399.
- [17] H. Dong, H. Zheng, L. Lin, B. Ye, Determination of thallium and cadmium on a chemically modified electrode with Langmuir–Blodgett film of p-allylcalix [4] arene, *Sensor. Actuator. B Chem.* 115 (2006) 303–308.
- [18] B. Karbowska, T. Rebiś, G. Milczarek, Electrode modified by reduced graphene oxide for monitoring of total thallium in grain products, *Int. J. Environ. Res. Publ. Health* 15 (2018) 653.
- [19] A. Söldner, J. Zach, B. König, Deep eutectic solvents as extraction media for metal salts and oxides exemplarily shown for phosphates from incinerated sewage sludge ash, *Green Chem.* 21 (2019) 321–328.
- [20] M. Baghayeri, A. Amiri, H. Razghandi, Employment of Pd nanoparticles at the structure of poly aminohippuric acid as a nanocomposite for hydrogen peroxide detection, *J. Electroanal. Chem.* 832 (2019) 142–151.
- [21] B. Uslu, H.Y. Aboul-Enein, S.A. Ozkan, Modern analytical electrochemistry: fundamentals, experimental techniques, and applications, *Int.J.Electrochem.Sci.* 2011 (2011).
- [22] B. Maleki, M. Baghayeri, M. Ghanei-Motlagh, F.M. Zonoz, A. Amiri, F. Hajizadeh, A. Hosseiniifar, E. Esmaeilnezhad, Polyamidoamine dendrimer functionalized iron oxide nanoparticles for simultaneous electrochemical detection of Pb^{2+} and Cd^{2+} ions in environmental waters, *Measurement* 140 (2019) 81–88.
- [23] B. Bansod, T. Kumar, R. Thakur, S. Rana, I. Singh, A review on various electrochemical techniques for heavy metal ions detection with different sensing platforms, *Biosens. Bioelectron.* 94 (2017) 443–455.
- [24] W. Zhang, L. Wang, Y. Yang, P. Gaskin, K.S. Teng, Recent advances on electrochemical sensors for the detection of organic disinfection byproducts in water, *ACS Sens.* 4 (2019) 1138–1150.
- [25] I. Bontidean, C. Berggren, G. Johansson, E. Csöregi, B. Mattiasson, J.R. Lloyd, K.J. Jakeman, N.L. Brown, Detection of heavy metal ions at femtomolar levels using protein-based biosensors, *Anal. Chem.* 70 (1998) 4162–4169.
- [26] M. Baghayeri, H. Alinezhad, M. Fayazi, M. Tarahomi, R. Ghanei-Motlagh, B. Maleki, A novel electrochemical sensor based on a glassy carbon electrode modified with dendrimer functionalized magnetic graphene oxide for simultaneous determination of trace Pb (II) and Cd (II), *Electrochim. Acta* 312 (2019) 80–88.
- [27] T. Kokab, A. Shah, F.J. Iftikhar, J. Nisar, M.S. Akhter, S.B. Khan, Amino acid-fabricated glassy carbon electrode for efficient simultaneous sensing of zinc(II), cadmium(II), copper(II), and mercury(II) ions, *ACS Omega* 4 (2019) 22057–22068.
- [28] T. kokab, A. Shah, J. Nisar, A.M. Khan, S.B. Khan, A.H. Shah, Tripeptide derivative-modified glassy carbon electrode: a novel electrochemical sensor for sensitive and selective detection of Cd^{2+} ions, *ACS Omega* 5 (2020) 10123–10132.
- [29] C.J. Siddons, *Metal Ion Complexing Properties of Amide Donating Ligands*, Citeseer, 2004.
- [30] H. Yuan, W. Ji, S. Chu, Q. Liu, S. Qian, J. Guang, J. Wang, X. Han, J.-F. Masson, W. Peng, Mercaptopyridine-functionalized gold nanoparticles for fiber-optic surface plasmon resonance Hg^{2+} sensing, *ACS Sens.* 4 (2019) 704–710.
- [31] M. Baghayeri, A. Amiri, B. Maleki, Z. Alizadeh, O. Reiser, A simple approach for simultaneous detection of cadmium (II) and lead (II) based on glutathione coated magnetic nanoparticles as a highly selective electrochemical probe, *Sensor. Actuator. B Chem.* 273 (2018) 1442–1450.
- [32] E. Khatiwora, P. Joshi, V. Puranik, D. Darmadhikari, A. Athawale, N.R. Deshpande, R. Kashalkar, Synthesis, characterization and bioactivity study of novel benzamides and their copper and cobalt complexes, *Int. J. Chem. Sci.* 11 (2013) 12–28.
- [33] D. Oltmanns, M. Eisenhut, W. Mier, U. Haberkorn, Benzamides as melanotropic carriers for radioisotopes, metals, cytotoxic agents and as enzyme inhibitors, *Curr. Med. Chem.* 16 (2009) 2086–2094.
- [34] G.R. Bardajee, M. Mohammadi, H. Yari, A. Ghaedi, Simple and efficient protocol for the synthesis of benzoxazole, benzoimidazole and benzothiazole heterocycles using Fe(III)–Schiff base/SBA-15 as a nanocatalyst, *Chin. Chem. Lett.* 27 (2016) 265–270.
- [35] Muhammad Ikram, Laifeng Ma, Xueyi Zhang, Mohib Ullah, Hongyuan Wu, Keying Shi, Controllable synthesis of an intercalated ZIF-67/EG structure for the detection of ultratrace Cd^{2+} , Cu^{2+} , Hg^{2+} and Pb^{2+} ions, *Chem. Eng. J.* 395 (2020) 125216–125228, <https://doi.org/10.1016/j.cej.2020.125216>.
- [36] Y. Wu, X. Han, Y. Qu, K. Zhao, C. Wang, G. Huang, H. Wu, Two Cu(I) complexes constructed by different N-heterocyclic benzoxazole ligands: syntheses, structures and fluorescent properties, *J. Mol. Struct.* 1191 (2019) 95–100.
- [37] Z.W. Peng, D. Yuan, Z.W. Jiang, Y.F. Li, Novel metal-organic gels of bis(benzimidazole)-based ligands with copper(II) for electrochemical selective sensing of nitrite, *Electrochim. Acta* 238 (2017) 1–8.
- [38] M. Haga, 1,8 - benzimidazole ligands, in: J.A. McCleverty, T.J. Meyer (Eds.), *Comprehensive Coordination Chemistry II*, Pergamon, Oxford, 2003, pp. 125–134.
- [39] K. Sone, Y. Fukuda, Y. Fukuda, *Inorganic Thermochromism*, Springer, 1987.
- [40] S. Pal, B. Manjunath, S. Ghorai, S. Sasmal, Chapter two - benzoxazole alkaloids: occurrence, Chemistry, and biology, in: H.-J. Knölker (Ed.), *The Alkaloids Chem. Biol.*, Academic Press, 2018, pp. 71–137.
- [41] H. Wang, L. Li, X. Zhang, S. Zhang, Polyamide thin-film composite membranes prepared from a novel triamine 3, 5-diamino-N-(4-aminophenyl)-benzamide monomer and m-phenylenediamine, *J. Membr. Sci.* 353 (2010) 78–84.
- [42] P. Chen, R.L. McCreery, Control of electron transfer kinetics at glassy carbon electrodes by specific surface modification, *Anal. Chem.* 68 (1996) 3958–3965.
- [43] G. Liu, J. Liu, T. Böcking, P.K. Eggers, J.J. Gooding, The modification of glassy carbon and gold electrodes with aryl diazonium salt: the impact of the electrode materials on the rate of heterogeneous electron transfer, *Chem. Phys.* 319 (2005) 136–146.
- [44] S. Yang, M. Yang, X. Yao, H. Fa, Y. Wang, C. Hou, A zeolitic imidazolate framework/carbon nanofiber nanocomposite based electrochemical sensor for simultaneous detection of co-existing dihydroxybenzene isomers, *Sensor. Actuator. B Chem.* 320 (2020) 128294.
- [45] V.W. Hung, A.J. Veloso, A.M. Chow, H.V. Ganesh, K. Seo, E. Kendüzler, I.R. Brown, K. Kerman, Electrochemical impedance spectroscopy for monitoring caspase-3 activity, *Electrochim. Acta* 162 (2015) 79–85.
- [46] T.S. Zeleke, M.-C. Tsai, M.A. Weret, C.-J. Huang, M.K. Birhanu, T.-C. Liu, C.-P. Huang, Y.-L. Soo, Y.-W. Yang, W.-N. Su, Immobilized single molecular molybdenum disulfide on carbonized polyacrylonitrile for hydrogen evolution reaction, *ACS Nano* 13 (6) (2019) 6720–6729, <https://doi.org/10.1021/acsnano.9b01266>.
- [47] D. Svehkarev, B. Dereka, A. Doroshenko, Mercury ions complexation with a series of heterocyclic derivatives of 3-hydroxychromone: spectral effects and prospects for ultrasensitive Hg^{2+} probing, *J. Phys. Chem.* 115 (2011) 4223–4230.